

See discussions, stats, and author profiles for this publication at: <https://www.researchgate.net/publication/253295761>

# Low-Frequency Amide Modes in Different Hydrogen-Bonded Forms of Nylon6 Studied by Inelastic Neutron Scattering and Density-Functional Calculations

ARTICLE *in* MACROMOLECULES · MAY 2002

Impact Factor: 5.8 · DOI: 10.1021/ma011218o

---

CITATIONS

17

---

READS

8

2 AUTHORS, INCLUDING:



[N. Sanjeeva Murthy](#)

Rutgers, The State University of New Jersey

212 PUBLICATIONS 3,517 CITATIONS

SEE PROFILE

# Low-Frequency Amide Modes in Different Hydrogen-Bonded Forms of Nylon-6 Studied by Inelastic Neutron Scattering and Density-Functional Calculations

**P. Papanek**

*Department of Materials Science and Engineering and Laboratory for Research on the Structure of Matter University of Pennsylvania, Philadelphia, Pennsylvania 19104; and NIST Center for Neutron Research National Institute of Standards and Technology Gaithersburg, Maryland 20899*

**J. E. Fischer\***

*Department of Materials Science and Engineering and Laboratory for Research on the Structure of Matter University of Pennsylvania, Philadelphia, Pennsylvania 19104*

**N. S. Murthy**

*Honeywell International, Inc., P.O. Box 1021R, Morristown, New Jersey 07962*

*Received July 12, 2001; Revised Manuscript Received January 24, 2002*

**ABSTRACT:** Inelastic neutron-scattering spectra of oriented nylon-6 were measured using the filter-analyzer and time-of-flight techniques. The samples studied were semicrystalline fibers with the crystalline fraction either in the  $\alpha$  or the  $\gamma$  form, and selectively deuterated polymer films. Strong features observed in the inelastic spectra correspond to vibrations of methylene groups, however several of the typical amide modes are also identified. The frequencies of observed amide V, VI and VII modes depend on the type of crystal structure. The lowest amide VII mode is located at 27 meV in the  $\alpha$  phase, and at 32 meV in the  $\gamma$  phase. Broad boson peaks are observed in both types of fibers, and attributed to their amorphous fractions. The boson peak of the  $\gamma$  fiber is found at a slightly higher frequency, which we explain by a higher cohesive energy density due to stronger hydrogen bonds or their higher density in the  $\gamma$  amorphous phase. Density functional calculations, using the B3LYP functional, were employed to study the vibrational modes of smaller model molecules, including H-bonded couples. These calculations show that hydrogen bonding significantly modifies not just the frequencies of out-of-plane amide vibrations, but the character of mode polarization vectors as well.

## I. Introduction

The polymer nylon-6,  $(-(\text{CH}_2)_5-\text{NHCO}-)_n$ , belongs to the family of nylons, or polyamides, characterized by the presence of secondary amide groups  $-\text{NHCO}-$  in the polymer skeleton. Consequently, hydrogen bonds can be formed between neighboring chains, which strongly affects the mechanical properties of these materials.

The secondary amide groups produce typical localized vibrational modes, traditionally referred to as amide I, II, III, ... modes that provide clear identification marks of these groups in the infrared (IR) and Raman spectra of polyamides. Although numerous studies of the vibrational properties of these polymers were performed using optical spectroscopic methods,<sup>1</sup> very little experimental work has been done using inelastic neutron scattering (INS). However, INS spectroscopy is well suited for the study of low-frequency modes, particularly those not easily accessible by optical methods. Furthermore, due to the large incoherent scattering cross-section of hydrogen, amide modes which involve considerable displacements of hydrogen atoms (i.e., protons that participate in the hydrogen bonding) should be readily observable. The study of amide dynamics is also of importance for a better understanding of the behavior of biological macromolecules, since the  $-\text{NHCO}-$  groups are the principal linkages in proteins and polypeptides and the hydrogen bonding between them directly affects their secondary structure.

Nylon-6 can crystallize in two different forms,  $\alpha$  and  $\gamma$ , identified by their distinct X-ray diffraction patterns. The availability of two different structural types allows us to investigate the effects of different chain conformations, and resulting different arrangements of H-bonds, on the vibrational modes. In the thermodynamically most stable  $\alpha$  form, the polymer chains are in the extended planar conformation. Neighboring chains are arranged in sheets of parallel but oppositely directed molecules. The crystal structure is monoclinic, and the chain axis repeat distance is  $b = 17.24 \text{ \AA}^2$ . In the  $\gamma$  form, the chains are in a twisted helical conformation, i.e., the plane of the secondary amide group is at  $66^\circ$  dihedral (torsional) angle with respect to the plane of the  $\text{CH}_2$  zigzag. The  $\gamma$  chains form sheets of parallel molecules joined by hydrogen bonds. The chain directions are opposite in alternating sheets. The crystal structure of the  $\gamma$  form is also monoclinic, but due to the nonplanar chain conformation the lattice parameter along the polymer axis is slightly shorter,  $b = 16.88 \text{ \AA}^3$ . The  $\gamma$  form can be produced by various methods, e.g., by high-speed spinning/drawing<sup>4,5</sup> or by iodinating the polymer, followed by the removal of iodine (see ref 6).

Recently, we have reported the medium-frequency INS spectra of the  $\alpha$  form of nylon-6.<sup>7</sup> Most of the modes observed in these experiments were in very good agreement with previous infrared (IR) and Raman measurements, but we were also able to identify normal modes not detected before by optical methods. Furthermore, by using an oriented sample (hot-drawn  $(4.5\times)$  fiber) it

was possible to discriminate between vibrational modes with hydrogen displacements perpendicular to polymer axes and modes parallel to polymer axes. Such "polarization information" allowed us to clarify the character of vibrational eigenmodes.

In this work, we present new results of inelastic neutron-scattering experiments on oriented fibers of both  $\alpha$  and  $\gamma$  crystalline forms of nylon-6. Two different methods, filter-analyzer neutron spectroscopy (using both Cu and pyrolytic graphite (PG) monochromators) and the time-of-flight technique, were used to extend the energy transfer (phonon frequency) range to 0–125 meV i.e., 0–1000  $\text{cm}^{-1}$  (1 meV = 8.066  $\text{cm}^{-1}$ ). Presented data essentially complete the available experimental information on the vibrational dynamics of nylon-6. To the best of our knowledge, these are also the first direct observations of the low-frequency amide modes (amide VII) in both crystalline forms of this polymer.

The strength of hydrogen bonding and its effects on the vibrational properties were also studied theoretically by first-principles calculations within the density-functional formalism. These calculations were carried out using the hybrid B3LYP functional for short model molecules containing the secondary amide groups. Among several models, we have also considered a couple of chain segments at different relative orientations to each other.

## II. Experimental Section

Semicrystalline fibers of  $\alpha$  and  $\gamma$  forms of nylon-6, used in these experiments, were obtained from Honeywell International Inc. The round cross-section fibers were hot drawn (4.5 $\times$ ), which induces anisotropy in the crystalline phase and a preferred orientation of polymer chains along the draw direction. The degree of crystallinity and orientation were determined as in previous wide-angle X-ray diffraction studies.<sup>10</sup> The  $\alpha$  fiber is about 47% crystalline and the orientational spread of the crystalline phase is  $\sim 14^\circ$ . The crystallinity and orientation of the  $\gamma$  fiber that we used were lower than in the  $\alpha$  fiber.

The  $\gamma$  form was produced from the drawn  $\alpha$  fiber by the commonly used KI/I<sub>2</sub> procedure.<sup>5</sup> The fiber was soaked overnight in an aqueous solution of 1.23 N KI and 1.23 N I<sub>2</sub>. It was then continuously rinsed with water for several minutes to remove excess iodine from the surface. This fiber was immersed in  $\sim 0.1$  M aqueous solution of sodium thiosulfate for several days, with the bath replenished several times with fresh solution, until almost all the complexed iodine was removed. The  $\gamma$  form prepared chemically by this method is similar to that obtained during the commercial high-speed spin-draw process, except that there is no trace of the  $\alpha$  crystalline form in the chemically produced fiber, and the lattice distortion is much less than in the commercial fiber.<sup>4,8</sup>

In our INS experiments, we used  $\sim 400$  mg of the  $\alpha$  and  $\gamma$  nylons. The fibers were wound on thin aluminum frames in such a way that the orientation was preserved and the chain axis (the crystallographic  $b$  axis) was parallel to one side of the frame. The wound packets were sealed in cylindrical Al containers filled with He gas.

Due to the high hydrogen content in the polymer, the inelastic scattering is almost exclusively incoherent and directly related to the amplitude-weighted vibrational density of states. The polarization discrimination is achieved by performing the measurements in two distinct scattering geometries, for which the wave-vector transfer  $\mathbf{Q}$  is either mainly perpendicular or parallel to the chain axis (the  $b$  axis) of the oriented polymer. The spectra obtained in  $Q \perp b$  ( $Q \parallel b$ ) then reflect the contribution of vibrational modes with displacements perpendicular (parallel) to chain axes. A detailed description of the experimental setup is given in our neutron-scattering study of stretch-oriented poly( $p$ -phenylene vinylene).<sup>11</sup>

Because in nylon-6 the ratio of hydrogen atoms present in the methylene groups and secondary amide groups is 10:1, the INS spectra will be dominated by vibrations involving CH<sub>2</sub> motions (either proper vibrations of methylene groups, or such vibrations of chain segments in which CH<sub>2</sub> groups are moving as almost rigid units). To amplify scattering features that originate from amide vibrations, additional experiments were performed on a selectively deuterated sample. In this sample, all hydrogen was replaced by deuterium except in the secondary amide groups. Since the incoherent scattering cross-section of deuterium,  $\sigma_{\text{inc}}(\text{D}) = 2.05$  b, is much smaller than the cross-section of H,  $\sigma_{\text{inc}}(\text{H}) = 80.27$  b (1 b =  $10^{-24}$  cm<sup>2</sup>), the relative intensity of peaks due to  $-\text{NHCO}-$  motions will be significantly stronger. This sample, referred to as NH-protonated nylon-6,  $(-\text{CD}_2)_5-\text{NHCO}-$ , was produced in the form of stretched films with the crystalline fraction in the thermodynamically stable  $\alpha$  form. The degree of orientation in these films was lower than in the fibers. The degree of deuteration of the methylene groups was  $\sim 90\%$ . About 300 mg of these films, mounted in a sample container similar to that used for the fully protonated fibers, were used in the neutron-scattering experiments.

INS spectra were collected using two different instruments: the filter-analyzer neutron spectrometer (FANS) and the time-of-flight (TOF) Fermi chopper spectrometer, both installed at the NIST Center for Neutron Research. FANS measurements were performed using a combined Be/graphite low-pass Bragg cutoff filter with an effective resolution  $\sim 1.2$  meV at low energies. A copper Cu(220) monochromator was used to cover the energy range 35–125 meV, and a pyrolytic graphite PG(002) monochromator was employed for the energy range 12–40 meV. The FANS spectra were recorded by scanning the neutron incident energy, and detecting all scattered neutrons through the low-pass filter for a fixed monitor count of incident neutrons.

The inelastic scattering at lower energies was measured using the Fermi chopper cold-neutron time-of-flight instrument. In this spectrometer, a set of monochromators selects the incident neutron wavelength 4.8 Å, and a rotating Fermi chopper with curved slots produces monochromatic pulses that hit the sample at precise time intervals. The scattered neutrons are detected by an array of detectors arranged at a fixed distance from the sample, and by measuring the flight time of neutrons, their final energy can be determined. The energy resolution is about 150  $\mu\text{eV}$  near zero energy transfer. From the set of neutron counts in all detectors and for all time channels, the scattering function  $S(\mathbf{Q}, E)$  can be derived by a straightforward procedure.

More detail about these techniques can be found in refs 11 and 12. In all inelastic spectra presented in this work (both FANS and TOF), the scattering due to the empty sample container was subtracted from the data.

## III. Results

**A. FANS Spectra.** Initial FANS measurements of the nylon-6  $\gamma$  fiber were performed under similar conditions as in our earlier study of the  $\alpha$  form.<sup>7</sup> The scattering from the oriented fibers was measured at 150 K in both scattering geometries ( $Q \perp b$  and  $Q \parallel b$ ). We found that the spectra of both  $\alpha$  and  $\gamma$  fibers, obtained in  $Q \perp b$ , are very similar, although the spectra of the  $\gamma$  form were noticeably noisier due to lower crystallinity and orientation of the sample. The most pronounced peaks in the  $Q \perp b$  polarization were found at 91, 101, and 118 meV, and assigned to CH<sub>2</sub> rocking and twisting vibrations. These normal modes are well-known from previous studies and they will not be discussed here in more detail.

The parallel spectra ( $Q \parallel b$ ) of the  $\alpha$  and  $\gamma$  forms of nylon-6, measured at 150 K, are shown in Figure 1, parts a and b, respectively. Three well-defined parallel modes are located at 46, 54, and 65 meV in the lower-frequency part of both figures. These modes have been

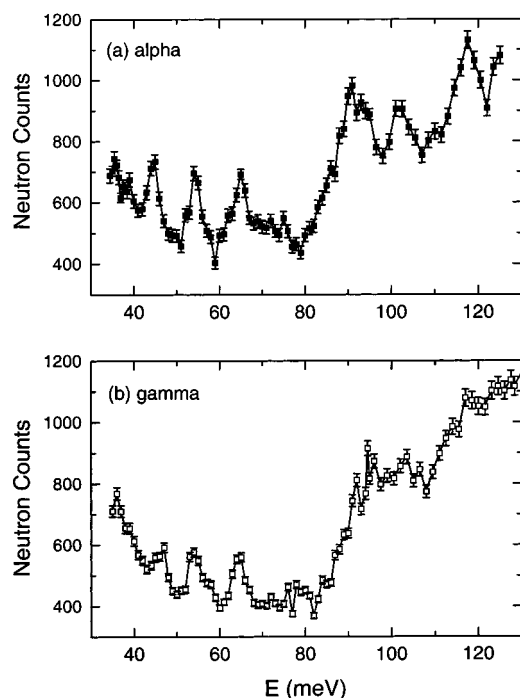


**Figure 1.** FANS spectra of oriented nylon-6 fibers measured at 150 K in the  $Q\parallel b$  scattering geometry: (a)  $\alpha$  form; (b)  $\gamma$  form.

analyzed in our earlier paper, and they are assigned to longitudinal skeletal deformations.<sup>7</sup> Their origin in nylons is explained by the splitting of the longitudinal acoustic phonon band of polyethylene chain  $(CH_2)_n$  into several optical bands due to a periodic perturbation (the presence of the heavier amide groups  $-NHCO-$ ). The fact that these frequencies (with the exception of the lowest mode at about 44 and 46 meV for  $\alpha$  and  $\gamma$  respectively) are essentially the same for both crystalline forms implies that these vibrations are not sensitive to conformation, and the mass effect is the determining factor.

FANS experiments were repeated at a much lower temperature  $T = 12$  K with significantly longer counting times to reduce the statistical noise in these measurements. Because we wanted to explore the amide VI mode, which involves atomic displacements normal to chain axes, we chose the  $Q\perp b$  scattering geometry. Figure 2 shows the data from all-hydrogen  $\alpha$  and  $\gamma$  samples and the selectively deuterated ("NH-protonated") sample. All three samples display strong scattering near 90 meV, corresponding to  $CH_2$  rocking vibrations. The longitudinal modes (46, 54 and 65 meV) produce small peaks in this geometry due to sample mosaicity and the less than ideal orientation of our drawn fibers. The  $\alpha$  form shows a peak at 72 meV, and a shoulder at 87 meV. In accordance with previous spectroscopic work, these features are assigned to amide VI and amide V modes, i.e., out-of-plane bending of  $C=O$  and  $N-H$  bonds, respectively. On the other hand, the scattering spectra of the  $\gamma$  form (Figure 2b) display only a very small peak, corresponding to the amide VI mode, shifted to 78 meV. Such sensitivity of the amide VI frequency to different crystalline polymorphs has been observed in IR spectra as well, and was reported for nylon-6<sup>13</sup> and nylon-11.<sup>14</sup> With regard to the amide V mode, we assume that the  $N-H$  bending vibrations are similarly shifted to higher frequencies, and hence, they cannot be distinguished from the strong  $CH_2$  rocking modes.

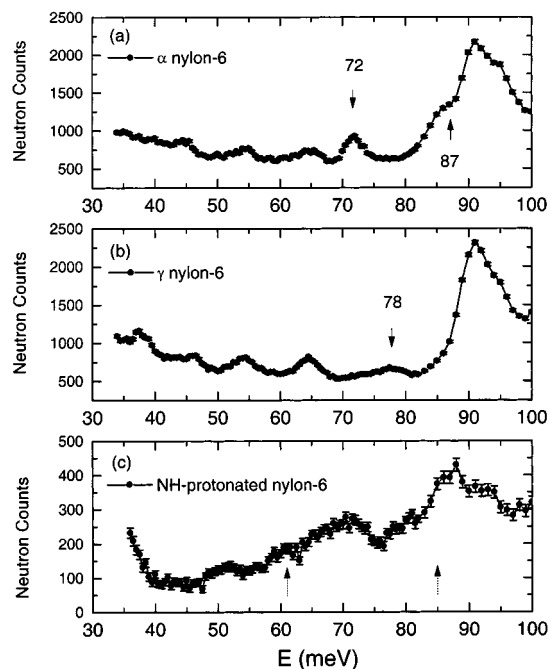


**Figure 2.** Low-temperature FANS spectra of oriented nylon-6 measured at 12 K in the  $Q\perp b$  geometry: (a)  $\alpha$  form; (b)  $\gamma$  form; (c) NH-protonated nylon-6. The dashed arrows in part c show where the two amide modes are expected upon deuteration of methylene groups.

The intensity of inelastic scattering from the NH-protonated nylon-6 (Figure 2c) is apparently much weaker due to its smaller mass and much lower hydrogen content. The interpretation of these data must be done very carefully. If the deuteration procedure was 100% effective (i.e., all  $CH_2$  groups replaced by  $CD_2$ ), we would expect the amide VI mode at  $\sim 61$  meV, and the amide V mode shifted only slightly to  $\sim 85$  meV. These frequencies, illustrated with dashed arrows in Figure 2c, are based on the results of vibrational calculations discussed in section IV, and also agree with results published in ref 15. At the same time, the  $CD_2$  rocking modes can be shifted to as low as 66 meV. Since only about 90% of methylene groups are in fact deuterated, the isotope shifts will be smaller and will vary, depending on the H/D ratio in chain segments. As a consequence, the scattering features are smeared out, particularly in the 60–70 meV region, which makes the identification of the amide modes very difficult. In any case, amide V mode should be very prominent, and the strongest scattering is indeed in the vicinity where this mode is expected.

The polarized FANS spectra in the 14–40 meV frequency range collected at  $T = 12$  K with  $Q\perp b$  are shown in Figure 3. Data (not shown) were also obtained in both  $Q\perp b$  and  $Q\parallel b$  modes in shorter runs at 150 K. Both  $\alpha$  and  $\gamma$  samples display broad maxima near 20 meV, polarized mainly perpendicular to the chain axis. The scattered intensity can be roughly approximated by a superposition of two peaks with positions at 17.5 and 21.5 meV in the  $\alpha$  form, and at 18 and 22 meV in the  $\gamma$  form. By comparison with the spectra of another crystalline polymer, polyacetylene  $(CH)_x$ , these features can be attributed to chain librations coupled to chain torsional vibrations.<sup>16</sup>

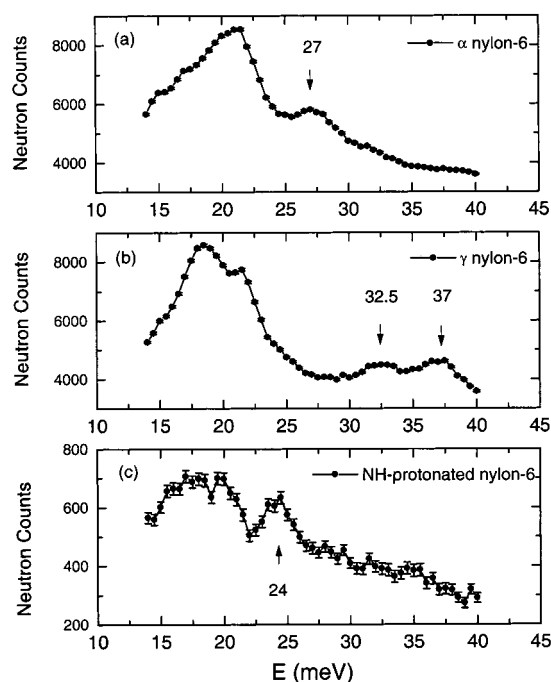
A smaller feature, located at 27 meV, is characteristic exclusively for the  $\alpha$  form, and is polarized perpendicular to chain- axis. On the other hand, the  $\gamma$  form shows



**Table 1.** Comparison of Neutron Scattering, Infrared, and Computational Results for Vibrational Modes in the  $\alpha, \gamma$  and NH-Protonated Forms of Nylon 6 (1 meV = 8.066 cm<sup>-1</sup>)<sup>a</sup>

amide modes	description	INS data			IR results				B3LYP calculations								
		$\alpha$	$\gamma$	NH	$\alpha$	$\gamma$	<b>1</b>	<b>2<math>\alpha</math></b>	<b>2 <math>\times</math> 2</b>	<b>2 <math>\times</math> 2</b>	<b>2<math>\gamma</math></b>	<b>2 <math>\times</math> 2</b>	<b>2 <math>\times</math> 2</b>	<b>3</b>	<b>3<math>\gamma</math></b>	<b>3<sub>NH</sub></b>	
									$\alpha$ -O	$\alpha$ -H		$\gamma$ -O	$\gamma$ -H				
I	$\nu(\text{CO})$				203.6	203.6	216.2	215.8			215.5			215.8	215.4	215.2	
II	$\delta(\text{NH}) + \nu(\text{CN})$				191.5	193.7	193.3	188.9			190.7			189.0	190.8	188.4	
III	$\delta(\text{NH}) + \nu(\text{CN})$				157.6	157.9	156.9	152.4			151.9			151.9	151.8	160.1	
IV	$\delta(\text{CO})$						77.1	81.7	81.3	81.5	87.0	88.4	91.6	81.3	87.2	73.8	
V	o/p $\gamma(\text{NH})$ bend	87	$\sim$ 90	$\sim$ 85	85.8	87.8	57.1	44.1	49.2	68.7	56.3	60.2	83.5	44.7	56.3	43.4	
VI	o/p $\gamma(\text{CO})$ bend	72	78	$\sim$ 60	71.8	77.2	78.8	73.6	73.7	79.5	72.8	72.0	73.2	73.7	73.6	62.3	
VII	o/p $\tau(\text{CN})$ torsion	27	32	24	27.4	34.0	21.1	12.5	13.8	14.5	12.4	13.1	13.4	19.3	10.2	16.3	
$Q\parallel b$	LO modes		36.5														
		44	46		45.9												
		54	54		55.4												
		65	65		64.8												
$Q\perp b$	chain torsion + librations	17.5	18	17													
		21.5	22	20													
$Q\perp b$	o/p chain deformation (O...H) stretch	$\sim$ 8	$\sim$ 8							8.2		10.5					
boson peak		2.6	3.2														

<sup>a</sup> IR results: amide I–V bands; ref 3; amide VI and VII bands, Matsubara and Magill (Matsubara, I.; Magill, J. H.; *J. Polym. Sci., Polym. Phys.* **1973**, *11*, 1173); LO modes, Tadokoro et al. H. (Tadokoro, H.; Kobayashi, M.; Yoshidome, H.; Tai, K.; Makino, D. *J. Chem. Phys.* **1968**, *49*, 339). B3LYP calculated frequencies are for molecules 1, 2, and 3 in the planar geometry, the nonplanar 2 $\gamma$  and 3 $\gamma$  molecules, and the selectively deuterated (NH-protonated) molecule 3NH. The Greek letters  $\nu$ ,  $\delta$ ,  $\gamma$ , and  $\tau$  in the second column denote bond stretching, in-plane bending, out-of-plane bending, and torsions, respectively. The column 2  $\times$  2 refers to the relaxed pairs of two planar  $\alpha$  and nonplanar  $\gamma$  conformers of **2** (Figure 5, parts a and c). The letters O or H in these columns refer to the vibrations of molecules whose O or H atoms participate in the hydrogen bond, respectively. Here, o/p is out of plane, and LO denotes a longitudinal optical mode of the polymer chain.

**Figure 3.** FANS spectra of oriented nylon-6 measured at 12 K in the  $Q\perp b$  geometry using PG(002) monochromator: (a)  $\alpha$  form; (b)  $\gamma$  form; (c) NH-protonated nylon-6.

peaks at 32.5 and 37 meV, almost equally strong in both polarizations. The inelastic spectrum of the NH-protonated sample is rather similar to that of the  $\alpha$  fiber, however the smaller peak is downshifted to 24 meV. Its significantly stronger relative intensity confirms that this is a peak associated with a vibrational mode of the secondary amide group. Fortunately, in this case there are no close methylene modes that would obscure the observation of this peak when downshifted upon deuteration. We assign these peaks to the amide VII mode, which can be to a first approximation thought of as a torsional vibration about the C–N bond. Thus, our data imply a lower frequency of this mode in the  $\alpha$  form (27

meV) than in the  $\gamma$  form (32.5 and 37 meV). We also note that while the polarization vectors for this mode are normal to the  $-\text{NHCO}-$  plane, they are not exclusively perpendicular to the chain axis for chains in the  $\gamma$  form, which explains the less polarized character of the scattering in our FANS data. The observed features are summarized in Table 1, together with the IR data from literature, and the time-of-flight results are discussed below.

**B. TOF Spectra.** All cold neutron time-of-flight experiments were carried out at the temperature 150 K. The  $Q\perp b$  geometry was realized in such a way that the  $b$  axis was normal to the scattering plane; i.e., the  $Q\perp b$  condition was satisfied for all scattering angles. This allows us to sum the response from most detectors (spanning the scattering angles  $25^\circ < \phi < 138^\circ$ ), which significantly improves signal-to-noise ratio in the data. To obtain the  $Q\parallel b$  geometry, the  $b$  axis has to lie in the scattering plane. Therefore, the samples were positioned with their  $b$  axes at  $45^\circ$  angle with respect to the incident beam, and only the data collected by detectors from the range  $89^\circ < \phi < 123^\circ$  (where the condition  $Q\parallel b$  is approximately satisfied) were considered. Since the selectively deuterated sample is a very weak scatterer, only the all-hydrogen polymers were measured with the TOF spectrometer.

Figure 4 shows the TOF-derived scattering functions  $S(Q, E)$  for the  $\alpha$  and  $\gamma$  forms in the perpendicular geometry (the data for the  $\alpha$  form are shifted upward for clarity). In both polarizations (data for parallel geometry not shown), the most pronounced features are the broad low-frequency boson peaks near 3 meV. Their presence in  $Q\perp b$  rules out the possibility that they originate from longitudinal chain-shearing vibrations in the crystalline regions, for example as in PPV.<sup>11</sup> The boson peak, as the name implies, is a feature that has an energy distribution proportional to Bose-Einstein statistics and is well-known from inelastic neutron and low-frequency Raman spectra of amorphous materials below the glass transition. It is usually found in the energy (frequency) range between 0.5 and 5 meV.<sup>17</sup> In

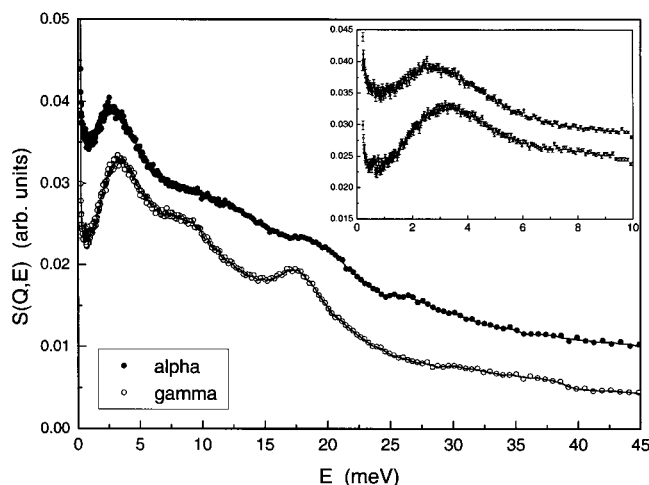


**Figure 4.** TOF-derived  $S(Q,E)$  for the  $\alpha$  (solid circles) and  $\gamma$  (open circles) forms of nylon-6 measured in the  $Q \perp b$  geometry. Data from detectors spanning the scattering angles  $25^\circ < \phi < 138^\circ$  were used.  $S(Q,E)$  of  $\alpha$  is shifted upward by 0.005 for clarity. The range 0–10 meV is shown enlarged in the inset.

our case, the assumption that the peaks near 3 meV originate in the amorphous phase explains the unpolarized character of the scattering, as well as the fact that the peak is more prominent in the less crystalline  $\gamma$  fiber. The precise origin of the boson peak is not well understood, and it has been attributed to localization of vibrational modes caused by the disorder in glassy materials.<sup>18</sup>

Curiously, the boson peak positions are different for  $\alpha$  and  $\gamma$  forms, as can be seen in the inset of Figure 4. The  $\alpha$  form frequency is 2.6 meV, whereas in the  $\gamma$  sample it is noticeably shifted to a higher frequency, 3.2 meV. In a recent neutron-scattering study of polyolefins, it has been suggested that the position of the boson peak correlates with the glass transition temperature and the cohesive energy density in chemically similar systems.<sup>19</sup> This would mean that the cohesive energy density in the amorphous phase of the  $\gamma$  fiber is greater than in the  $\alpha$  fiber, presumably because of higher density of hydrogen bonds. The qualitative difference between the amorphous phases of our  $\alpha$  and  $\gamma$  samples may be the result of the treatment procedure during the preparation of the  $\gamma$  fiber. Another explanation could be that the treatment caused rearrangement of chains in the amorphous phase such that stronger H-bonds could be formed.

The shoulder or peak that appears at  $\sim 8$  meV (Figure 4) must correspond to a perpendicularly polarized mode, since it is not resolved in the  $Q \parallel b$  spectra (data not shown). We assign it to chain translational vibrations and out-of-plane deformations of the (planar) methylene sequences. Due to its proximity to the broad low-frequency boson peak, it is however difficult to determine whether its frequency is indeed identical for both crystalline forms. The mode near 18 meV is also mainly perpendicular and produces the strong scattering in the FANS (PG monochromator) spectra discussed in the previous section. Features at 27 meV in  $\alpha$ , and between 32 and 37 meV in the  $\gamma$  sample, correspond to the amide VII modes already identified by FANS. Obviously, the FANS data are by far superior at these frequencies.

#### IV. Density-Functional Calculations

To gain more insight into the vibrational dynamics of  $\alpha$  and  $\gamma$  forms of nylon-6, we have performed

vibrational analysis of model compounds, using force constants calculated by density-functional methods. Density-functional (DF) theory takes into account electron correlation effects which play an important role in determining the properties of hydrogen-bonded system. One of the advantages (and reasons of popularity) of DF calculations is that they are orders of magnitude faster than the conventional post-Hartree–Fock many-body perturbation methods.

Various exchange and correlation functionals have been developed in the DF theory in recent years. The combination of Becke's three-parameter exchange functional<sup>20</sup> and Lee–Yang–Parr correlation functional,<sup>21</sup> known as B3LYP, has satisfactorily predicted the energies and molecular geometries of several hydrogen-bonded systems that involve the secondary amide groups.<sup>22</sup> Therefore, we have chosen this functional in all of our DF calculations, together with the large basis set 6-311++G(d,p), implemented in the quantum chemistry software package Gaussian 94.<sup>23</sup>

**A. Single Molecule Calculations.** The following model molecules, containing the secondary amide groups, were considered for the vibrational analysis: (1) *N*-methyl acetamide,  $\text{CH}_3\text{—NHCO—CH}_3$ , (2) *N*-ethyl propionamide,  $\text{CH}_3\text{—CH}_2\text{—NHCO—CH}_2\text{—CH}_3$ , (3) *N*-propyl propionamide,  $\text{CH}_3\text{—(CH}_2)_2\text{—NHCO—CH}_2\text{—CH}_3$ , and a hydrogen-bonded pair of molecule **2** at different relative orientations. Rather than search for all low-energy conformations, we have concentrated only on those which are close to the geometry of chain segments in the two crystal structures of nylon-6. We also note that calculations for larger segments of the nylon-6 chain or the full periodic 3-dimensional crystal would require an extremely large amount of CPU resources even on high-performance computers.

After the molecular geometry of each compound was optimized to an equilibrium (local energy minimum) point, the force constants were calculated by numerical differentiation of analytical first derivatives of potential energy with respect to nuclear coordinates. Conformation of the extended  $\alpha$  chains was optimized by imposing  $C_s$  symmetry wherein the C atoms of the alkyl groups lie in the plane of the  $\text{—NHCO—}$  group. We have also attempted to optimize a nonplanar geometry, similar to chain conformation in the  $\gamma$  crystal, for compounds **2** and **3**, and such relaxed geometries were indeed found. However, there are small differences between the calculated “ $\gamma$ -like” conformers (labeled as  $2\gamma$  and  $3\gamma$  in the following) and the local chain geometry in the  $\gamma$  nylon-6 crystal. Most importantly, the dihedral (torsional) angles of the bonded sequence  $\text{C—C—N—C(O)}$  and  $\text{N—C(O)—C—C}$  in the  $2\gamma$  molecule are  $+92.8$  and  $-139.7^\circ$ , respectively ( $+92.3$  and  $-139.1^\circ$  in the  $3\gamma$  conformer), whereas similar dihedral angles are  $\pm 114.1^\circ$  in the  $\gamma$  crystal (of course, in the planar  $\alpha$ -like conformation, these angles are  $\pm 180^\circ$ ).

The calculated mode frequencies of amide I ( $\text{C=O}$  stretch), amide II (in-plane  $\text{N—H}$  bend coupled with  $\text{C—N}$  stretch), amide III (coupled  $\text{N—H}$  bend and  $\text{C—N}$  stretch as in amide II, but in an opposite phase), amide IV (in-plane  $\text{C=O}$  bend), amide V (out-of-plane  $\text{N—H}$  bend), amide VI (out-of-plane  $\text{C=O}$  bend), and amide VII (out-of-plane  $\text{C—N}$  torsions) for all model molecules are given in Table 1. The higher-frequency modes were included for completeness and because of their particular importance in IR spectroscopy. To illustrate the effect of selective deuteration, the table also includes

calculated frequencies for compound **3** (in the  $\alpha$  geometry) with all hydrogen atoms replaced by deuterium except in the secondary amide group (denoted as **3**NH).

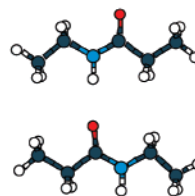
The calculated frequencies of amide I, II, and III modes show only very weak dependence on the molecular size and conformation. Whereas results for the amide I mode (C=O stretch) are about 12 meV greater than the experimental value for nylon-6 (~203 meV) amide II and III results are close to observed frequencies (in nylon-6, these modes are at 192.3 and 158.7 meV, respectively<sup>1,15</sup>).

According to the B3LYP calculations, the amide IV mode (in plane C=O bend) is quite sensitive to molecular geometry, and its frequency should be higher for  $\gamma$  conformations. There is little experimental data to confirm this trend. Our inelastic neutron spectra did not reveal this mode, because the vibration does not involve significant hydrogen motions and hence the intensity is weak. INS spectra of crystalline *N*-methyl acetamide (compound **1**) do not reveal this mode either, but it is well resolved in IR spectra at 79.3 meV, close to amide VI (out-of-plane C=O bend) at ~74.4 meV.<sup>24</sup> Our B3LYP results are in satisfactory agreement with these numbers, however the frequencies are in a reverse order (amide VI higher than amide IV for molecule **1**). A possible explanation could be that these single molecule calculations neglect the effects of intermolecular hydrogen bonding. We will return to this point in the discussion of results for hydrogen-bonded pairs.

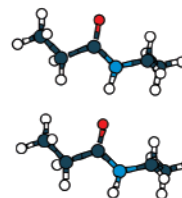
The out-of-plane N–H bending modes (amide V) are computed in the interval 43–57 meV. The frequencies show strong sensitivity to the molecular geometry, and are about 12 meV higher for the  $\gamma$  conformations. This result was expected. But, the calculated numbers are surprisingly low—amide V modes are usually observed in the 87 meV region, and our INS spectra also suggest that this mode is at 87 meV and at (90 meV) in the  $\alpha$  and  $\gamma$  nylon-6 fibers, respectively. A combined neutron-scattering and ab initio modeling study of solid *N*-methyl formamide (NMF, CH<sub>3</sub>–NHCO–H) revealed a similar behavior.<sup>25</sup> The N–H bending mode of a single molecule is calculated at 58.4 meV, but when two or several NMF molecules are associated by hydrogen bonds, the calculated vibrations are shifted to a much higher frequency 89.5 meV, closer to the experimentally observed value 96 meV. Clearly, there is a strong hydrogen-bonding effect on the amide V mode.

Both amide VI and VII modes are also out-of-plane vibrations, but with significant displacements of oxygen atoms in the former, and nitrogen atoms in the latter. B3LYP amide VI frequencies are in good agreement with our INS data which locate this mode at 72 meV (72 meV) in the  $\alpha$  form. On the other hand, the calculations fail to reproduce the observed ~6 meV shift to a higher frequency in the  $\gamma$  form. Selective deuteration as in the **3**NH molecule causes a downshift of this mode corresponding to the frequency ratio ~0.85; when applied to the experimental value, this predicts the amide VI vibration near ~61 meV in the NH-protonated nylon-6 (shown with a dashed arrow in Figure 2c). Analogous ratio for the frequency of the strong rocking modes (CD<sub>2</sub> rock/CH<sub>2</sub> rock), calculated by B3LYP for molecule **3**, is about 0.73 (68.4 meV/94.0 meV), which gives an expected shift from 91 to ~66 meV, and consequently makes a direct observation of the amide VI mode in the NH-protonated sample very difficult.

(a) " $\alpha$ " orientation, final



(b) " $\gamma$ " orientation, initial



(c) " $\gamma$ " orientation, final

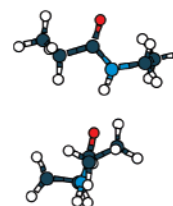


**Figure 5.** Illustrations of molecular geometries considered in the density-functional B3LYP calculations: (a) optimized pair of antiparallel planar molecules **2**; (b) initial orientation of two  $2\gamma$  molecules, with their amide groups placed in the same plane; (c) relaxed geometry of the pair of  $2\gamma$  molecules. The molecules are rotated such that the angle between the amide planes is ~90°.

The amide VII mode is generally described as a C–N torsional vibration. Its calculated value is lower than the observed frequencies, and the  $\gamma$  conformation results are consistently smaller than the results for planar  $\alpha$  geometries, in a contradiction with experiment. We are aware of one study of *N*-methyl acetamide, where such a torsional vibration was assigned to an observed peak at 20.3 meV (very close to our calculated value 21.1 meV), and the amide VII mode was assigned to a weak feature at 38.3 meV and attributed to higher transitions of the torsional modes.<sup>26</sup> As was the case with the previous out-of-plane modes, it is necessary to study the influence of intermolecular H-bonding on this particular mode in more detail.

**B. Analysis of Hydrogen-Bonded Pairs.** To optimize a hydrogen-bonded geometry for the  $\alpha$  form, two planar molecules **2** were placed antiparallel to each other and lying on the same plane, as found in the  $\alpha$  crystal. The geometry was relaxed with no additional constraints, and the local energy minimum position readily obtained (Figure 5a). As a consequence of the H-bonding, the C=O and N–H bonds elongated from 1.222 to 1.227 Å, and from 1.008 to 1.014 Å, respectively. The hydrogen bonding distance O···H is 2.087 Å.

To optimize the hydrogen-bonded pair of  $\gamma$ -like molecules, two  $2\gamma$  conformers were initially placed parallel to each other, and with their –NHCO– groups lying in the same plane (Figure 5b). No symmetry constraints were employed during the B3LYP optimization. However, it was not possible to optimize an equilibrium geometry resembling the arrangement in the nylon-6  $\gamma$  crystal. Instead, the relaxed geometry of this pair,



shown in Figure 5c, is characterized by  $\sim 90^\circ$  angle between the planes of the two  $-\text{NHCO}-$  groups. The geometry of each of the molecules remained relatively unchanged, when compared to the optimized geometry of a single  $2\gamma$  conformer. This implies that the interactions between amide groups are the principal driving forces determining the relative orientation of the pair. Although the relative orientation of the pair of  $\gamma$  conformers, Figure 5c, does not correspond to the arrangement of chains in the nylon-6  $\gamma$  crystalline phase, such orientations (with the planes of secondary amide groups of neighboring chains perpendicular to each other) may occur easily in the amorphous phase.

The  $\text{C}=\text{O}$  and  $\text{N}-\text{H}$  bond lengths are 1.229 and 1.015 Å, respectively, and both bonds are slightly more elongated than in the “ $\alpha$  orientation”. The calculated hydrogen bonding distance  $\text{O}\cdots\text{H}$  is 2.001 Å. Hence, the calculated hydrogen bonding is stronger in the perpendicular arrangement of two  $2\gamma$  molecules than in the antiparallel orientation of two planar  $\alpha$  conformers. This conclusion is further supported by the comparison of interaction energies,  $\Delta E = E(\text{couple}) - 2E(\text{single})$ , for the  $\alpha$  and  $\gamma$  couples:  $\Delta E(\alpha \text{ couple}) = -4.87$  kcal/mol, and  $\Delta E(\gamma \text{ couple}) = -5.96$  kcal/mol. We note that these calculations give only crude estimates of the interaction energies, which may in fact depend somewhat on the extension of the applied atomic basis set. We also note that from the analysis of Fermi resonance bands in IR spectra of nylons it was deduced that the hydrogen bonds are weaker in the  $\alpha$  form than in the  $\gamma$  form, or the amorphous phase.<sup>13</sup> Hence, it appears that the B3LYP calculated interaction energies, although crude, agree with experimental findings.

A full vibrational analysis was carried out for the optimized geometry of the antiparallel pair of  $\alpha$  conformers, and for the relaxed  $\gamma$  pair. We are interested mainly in the modification of the low-frequency amide modes due to hydrogen bonding, and these modes are listed in Table 1. The H-bond stretching vibration, also listed in the table, is  $\sim 2.2$  meV higher in the  $\gamma$  pair, and this signifies that the corresponding minimum of the potential energy hypersurface is not only lower but also sharper (with respect to the intermolecular separation) for this configuration than for the  $\alpha$  pair. The amide IV mode is only very weakly affected by the hydrogen bond, whereas the out-of-plane amide V and VI modes are shifted to higher frequencies, especially for the molecule whose hydrogen atom takes part in the H-bonding. Whereas the amide V mode at 49.2 meV (Figure 6a), localized on the first molecule of the  $\alpha$  pair, resembles the pure N–H bending vibration as in an isolated molecule, such a vibration of the second molecule is coupled with out-of-plane motions of C atom of the carbonyl group, and the nearest  $\text{CH}_2$  group, as shown in Figure 6b. The calculated frequency (68.7 meV) still falls short of the observed value ( $\sim 87$  meV), but it can be assumed that if the amide groups were associated by H-bonds on both sides, the frequency shift would be even higher. Amide VI modes (Figure 6, parts c and d, for the  $\alpha$  couple) can be characterized as  $\text{C}=\text{O}$  out-of-plane bending coupled with N–H bending and  $\text{CH}_2$  rocking of the nearest methylene group. Even in this case, the frequency is higher for the amide group that has its H atom participating in the hydrogen bonding. We also note that the frequency change in the  $\gamma$  couple is quite small. The torsional amide VII modes are also weakly affected by hydrogen bonding. The

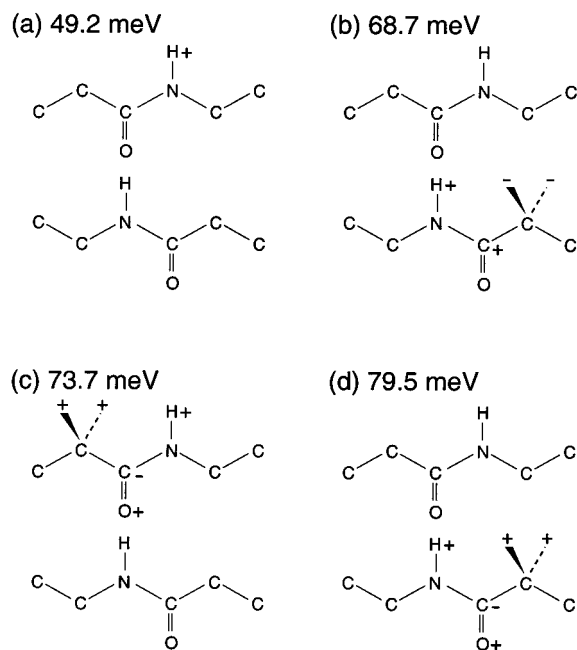


**Figure 6.** Schematic representations of the amide modes calculated by B3LYP for the hydrogen-bonded pair of planar molecules **2**. Parts a and b depict amide V; parts c and d depict amide VI modes. The + and – signs denote displacements normal to the plane.

calculated frequencies in the  $\alpha$  pair are higher than those in the  $\gamma$  pair, contrary to our conclusions from the experiments. We recall, however, that the relaxed geometry of the  $\gamma$  pair does not correspond to the geometry of bonded chains in  $\gamma$  nylon-6.

## V. Conclusions

One of the main objectives of this work was to investigate the effects of interchain interactions, and in particular hydrogen bonding, on the vibrational dynamics in different phases of the polymer nylon-6. To this end, we have performed inelastic neutron-scattering experiments on oriented fibers of the  $\alpha$  and  $\gamma$  forms of this polymer, using the filter-analyzer and neutron time-of-flight techniques.

Although the strongest features found in the inelastic spectra correspond to vibrational modes connected with methylene  $\text{CH}_2$  motions, the typical vibrations of the secondary amide groups were also identified. All of the observed low-frequency amide V, VI, and VII modes are characterized by out-of-plane deformations of the  $-\text{NHCO}-$  groups. They also display a significant dependence on the crystal structure, and the frequencies in the thermodynamically stable  $\alpha$  phase are lower than in the  $\gamma$  phase. This is true even for the torsional amide VII mode that is found at 27 meV in  $\alpha$  and between 32 and 37 meV in  $\gamma$  nylon-6. In our knowledge this is the first time such an observation is reported.

Density-functional calculations, based on Becke's exchange, and Lee–Yang–Parr correlation functionals provided important clues in the analysis of amide modes. While the results for isolated planar  $\alpha$ , and nonplanar  $\gamma$  conformers show that all amide modes are to a certain degree dependent on the molecular geometry, the out-of-plane amide vibrations are especially strongly modified when hydrogen bonds are formed between the  $-\text{NHCO}-$  groups. The most dramatic effect, according to these calculations, is on the N–H bending mode, which shifts by  $\sim 25$  meV. The agreement



between the calculated values and experimental data is good for the amide VI mode but poor for all the other bands since the calculations are performed for relatively small systems, and for example the effect of cooperative H-bonding, when several amide groups are associated with each other, is completely neglected.

At the very lowest frequencies, time-of-flight spectra display broad boson peaks in both  $\alpha$  and  $\gamma$  samples. These peaks, characteristic for the amorphous phase, occur at slightly different positions, which is attributed to higher cohesive energy density in the amorphous phase of the  $\gamma$  fiber due to either or both stronger hydrogen bonds and higher density.

**Acknowledgment.** We would like to thank B. Frick for helpful discussions, and D. Neumann, T. Udovic, and C. Brown for much good advice and assistance in these measurements. This work was supported by the NSF MRSEC Program under Grant No. DMR00-79909. The use of supercomputer facilities at NIST, and at the National Energy Research Scientific Computing Center is also acknowledged.

## References and Notes

- (1) Hendra, P. J.; Maddams, W. F.; Royand, I. A. M.; Willis, H. A.; Zichy, V. *Spectrochim. Acta* **1990**, 46A, 747 and references therein.
- (2) Holmes, D. R.; Bunn, C. W.; Smith, D. J. *J. Polym. Sci.* **1955**, 17, 159.
- (3) Arimoto, H.; Ishibashi, M.; Hirai, M.; Chatani, Y. *J. Polym. Sci. A* **1965**, 3, 317.
- (4) Murthy, N. S.; Aharoni, S. M.; Szollosi, A. B. *J. Polym. Sci., Polym. Phys.* **1985**, 23, 2549.
- (5) Salem, D. R.; Moore, R. A. F.; Weigmann, H. D. *J. Polym. Sci., Polym. Phys.* **1987**, 25, 567.
- (6) Arimoto, H. *J. Polym. Sci., Polym. Phys.* **1964**, 2, 2283.
- (7) Papenek, P.; Fischer, J. E.; Murthy, N. S. *Macromolecules* **1996**, 29, 2253.
- (8) Murthy, N. S. *J. Polym. Sci., Polym. Phys.* **1986**, 24, 549.
- (9) Murthy, N. S.; Minor, H.; Bednarczyk, C.; Krimm, S. *Macromolecules* **1993**, 26, 1712.
- (10) Murthy, N. S.; Bray, R. G.; Correale, S. T.; Moore, R. A. F. *Polymer* **1995**, 36, 3863.
- (11) Papenek, P.; Fischer, J. E.; Sauvajol, J. L.; Dianoux, A. J.; Mao, G.; Winokur, M. J.; Karasz, F. E. *Phys. Rev. B* **1994**, 50, 15668.
- (12) Copley, J. R. D.; Udovic, T. J. *J. Res. Natl. Inst. Stand. Technol.* **1993**, 98, 71.
- (13) Murthy, N. S.; Stamm, M.; Sibilia, J. P.; Krimm, S. *Macromolecules* **1989**, 22, 1261.
- (14) Balizer, E.; Fedderly, J.; Haught, D.; Dickens, B.; Deroggi, A. S. *J. Polym. Sci., Part B* **1994**, 32, 365.
- (15) Jakes, J.; Krimm, S. *Spectrochim. Acta* **1971**, 27A, 19.
- (16) Papenek, P.; Fischer, J. E.; Sauvajol, J. L.; Dianoux, A. J.; McNeillis, P. M.; Mathis, C.; Francois, B. In *Neutron Scattering in Materials Science*; Neumann, D. A., Russell, T. P., Wuensch, B. J., Eds; Materials Research Society Symposium Proceedings 376; Materials Research Society: Warrendale, PA, 1995; p 763.
- (17) Frick, B.; Richter, D. *Science* **1995**, 267, 1939.
- (18) Wischniewski, A.; Buchenau, U.; Dianoux, A. J.; Kamitakahara, W. A.; Zarestky, J. L. *Philos. Mag. B* **1998**, 77, 579.
- (19) Annis, B. K.; Lohse, D. J.; Trouw, F. *J. Chem. Phys.* **1999**, 111, 1699.
- (20) Becke, A. D. *J. Chem. Phys.* **1993**, 98, 5648.
- (21) Lee, C.; Yang, W.; Parr, R. G. *Phys. Rev. B* **1988**, 37, 785.
- (22) Han, W. G.; Suhai, S. *J. Phys. Chem.* **1996**, 100, 3942.
- (23) Frisch, M. J.; et al. Gaussian 94, Revision E.3. Gaussian Inc.: Pittsburgh, PA, 1995.
- (24) Barthes, M.; Bordallo, H. N.; Eckert, J.; Maurus, O.; de Nunzio, G.; Léon, J. *J. Phys. Chem. B* **1998**, 102, 6177.
- (25) Bouř, P.; Tam, C. N.; Sopková, J.; Trouw, F. R. *J. Chem. Phys.* **1998**, 108, 351.
- (26) Fillaux, F.; Fontaine, J. P.; Baron, M. H.; Kearly, G. J.; Tomkinson, J. *Chem. Phys.* **1993**, 176, 249.
- (27) Frick, B. Private communication.

MA011218O